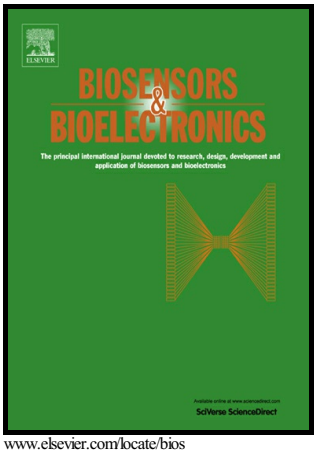

www.elsevier.com/locate/bios

Non-enzymatic sensing of glucose using screen-printed electrode modified with novel synthesized CeO_2@CuO core shell nanostructure

Dayakar T, K. Venkateswara Rao, K. Bikshalu, V. malapati, Kishor Kumar Sadasivuni

PII: S0956-5663(18)30250-1
DOI: https://doi.org/10.1016/j.bios.2018.03.063
Reference: BIOS10389

To appear in: *Biosensors and Bioelectronic*

Received date: 7 January 2018
Revised date: 11 March 2018
Accepted date: 28 March 2018

Cite this article as: Dayakar T, K. Venkateswara Rao, K. Bikshalu, V. malapati and Kishor Kumar Sadasivuni, Non-enzymatic sensing of glucose using screen-printed electrode modified with novel synthesized CeO_2@CuO core shell nanostructure, *Biosensors and Bioelectronic,* https://doi.org/10.1016/j.bios.2018.03.063

Non-enzymatic sensing of glucose using screen-printed electrode modified with novel synthesized CeO_2@CuO core shell nanostructure

Dayakar. T[a], K. Venkateswara Rao[a*], K. Bikshalu[b], V. malapati[c], Kishor Kumar Sadasivuni[d]

[a]*Center for Nanoscience and Technology, Institute of Science and Technology, Jawaharlal Nehru Technological University Hyderabad, Telangana State, 500085, India*

[b]*Department of Electronics & Communication Engineering, Kakatiya University, Warangal, Telangana State, 506009, India*

[c]*Department of Science & technology, Vignan foundation for Science, Technology & Research, Guntur, Andhra Pradesh-522213, India.*

[d]*Department of Mechanical and Industrial Engineering, Qatar University, Doha, Qatar-2713.*

*Corresponding author. Mobile No: +91-9440858664. kalagadda2003@gmail.com

Abstract

We fabricated a fourth generation glucose biosensor using CeO_2@CuO core shell nano structure (CeCCS NSs). A simple leave extract of *Ocimum tenuiflorum* was used to prepare different wt% of 0.2, 04, 0.6, and 0.8 CuO (shell), above 1 wt % of CeO_2 (core). The successful formation was confirmed by various characterization techniques like XRD, Uv-Vis, FTIR, SEM and HR-TEM. In the biosensor, 0.4 wt% of CeCCS NSs has shown efficient properties due to its high surface area. The good conductivity and high catalytic activity towards glucose sensing properties were estimated by screen-printed electrode (SPE). The ampherometric studies of CeCCS/SPE modified electrode have been optimized at potential +0.4 V, showed a sensitivity of 3319.83 $\mu AmM^{-1}cm^{-2}$ within detection limit of 0.019 µM. More significantly, modified electrodes performed excellently against anti-interference and anti-poisoned activity in glucose sample and exhibited promising results for the sustainable improvement for non-enzymatic sensing applications.

Keywords: Ocimum tenuiflorum, Core shell nanostructure, Electro catalytic activity and Non-enzymatic glucose sensor.

1. Introduction

The advantage of direct electron transfer mechanism for fourth generation biosensors have attracted research community in recent years, due to development of enzyme free biosensors electrodes [Yan et al., 2016]. The difficulty allied with these biosensors such as selectivity, electrode's slow kinetics, and the real time sample ingredient fouling prohibited these sensors from scientific and technical applications [Kun et al., 2014; Rahman et al., 2010]. To overcome these limitations, there is a need to fabricate enhanced electrode surface area, nano dimensional catalyst with low potential material [Shearer et al., 2016]. A combination of nanomaterials such as alloys, composites, core-shells proves these properties for potential applications. Among them the core-shell nano structures have fast electron transfer and protect the core from fouling and low glucose oxidation potential [Warren et al., 2012; Liu et al., 2009; Sun et al., 2011].

In our present study, copper oxide (CuO) has been considered as shell, because of its high catalytic activity with narrow band gap to promote affective glucose oxidation and also corrosion resistance to avoid anti interference and anti-poisoning effect with interference substances in glucose

solution [Heinemann et al., 2013; Balamurugan et al., 2001]. Copper oxide (CuO) will enhance the specificity of sensor, which were lack to exhibit by the core CeO_2, but interestingly, the core material show significant effect in our present study by having properties such as electron conduction suitable to induce electron transfer, chemical inertness, non-toxicity, bio-compatibility for glucose oxidation [Zhuang et al., 2018; Uzunoglu et al., 2016]. The catalytic activity of metal oxides is higher than pure metals of Cu or Cerium due to Cu atom interactions with oxide ion vacancies in cerium (Ce), this synergetic effect can be explained by the stabilization of Cu ions by ceria and enhanced active oxygen, which facilitates the formation of oxide ion vacancies [Trovarelli et al., 2001; Uzunoglu et al., 2015; Tschope et al., 1994], Thus the combination provides suitable sensing nano surface interface to enhance synergetic affect in materials for non-enzymatic application.

CeO_2@CuO core-shell nano structures (CeCCS NSs) have been synthesized from physical and chemical methods have been reported elsewhere, CeO_2-based core/shell nanoparticles have been synthesized using chemical precipitation method for oxygen storage capacity [Aytekin et al., 2013]. The Cu_2O@CeO_2 core-shell nanostructures with strong coupling have been synthesized by aqueous solution route for catalytic tests [Wang et al., 2015]. Enzyme free glucose sensors have been fabricated using CeO_2-CuO core shells prepared from wet impregnation method [Panpan et al., 2016]. Polyaniline/Cerium Oxide electrode was used for non-enzymatic glucose sensor [Jie et al., 2013]. Uric acid presence was confirmed in biological fluids by indium (In) doped CeO_2 nanoparticles [Yassien et al., 2016]. CuO/CeO_2 applied for catalytic applications [Paola et al., 2016], [Shanghong Zeng et al., 2014], [Shanghong Zeng et al., 2013], [Huizhi Bao et al., 2014], [A. Horne´s et al., 2009] and [Wei-guo Pan et al., 2013]. By understanding, very few reports are available on bio-mediated synthesis of core-shell nano structures from plants, bacteria, algae and fungi due to their eco-friendly reducing and stabilizing reaction activities.

The choice of the Ocimum tenuiflorum was mainly due to abundant, simple leaf structure to easy leaf extraction, and high medicinal value [Rupali et al., 2012]. Recent studies showed that O. tenuiflorum exhibited large amount of reducing and capping agents such as oleanolic acid, rosmarinic acid, linalool, ursolic acid, eugenol, β-caryophyllene, carvacrol, germacrene and terpenes. Among them, the active constituent is Eugenol (l-hydroxy-2-methoxy-4- allylbenzene) [John et al., 2016]. These compounds can easily reduce the size and can easily remove from surface of materials after calcinations, which improve the crystalinity without affecting the shape of nanoparticles. The possible mechanism involves the large group of flavonoids acts as reducing and stabilizing agents, which actively adsorbed on the surface, and form complex structure with nanoparticles. Simultaneous involves the transformation of flavonoids from ketones to carboxylic acids, which plays a key role in the reduction. Generally, the polyphenols and alkaloids prevent oxidation of NPs but it can be overcome by applying the temperature to reaction process for the formation of metal oxides.

In this work, we present a simple study on bio-mediated method to synthesize CeCCS NSs. As prepared CeCCS/SPE modified electrodes are applied for evaluation of non-enzymatic glucose sensing in alkali solution. The sensor shows an excellent selectivity against organic and inorganic compounds present in glucose solution with good sensitivity. It proved that, CeCCS NSs can have sustainable feature for non-enzymatic sensing applications.

2. Materials and Methods

2.1 Chemicals and apparatus

Copper(II) nitrate $Cu(NO_3)_2$, cerium nitrate $Ce(NO_3)_2$, Sodium hydroxide (NaOH), and inorganic and organic compounds were obtained from Sigma Aldrich and used as received and the Human blood serum was collected from volunteers. Ocimum tenuiflorum leaves have collected from greenhouse of CNST, IST, JNTUH, INDIA, which we specially grew up for the green synthesis of nanomaterials. Electrochemical studies were carried out on a AUTOLAB PGSTAT302N (potentiostat/galvanostat) equipped with a USB electrochemical interface and driven by a NOVA 2.0.2 software package (Eco Chemie, The Netherlands) in conjunction with a electrode strip connector and a personal computer for data storage and processing. The SPE integrated with three electrodes were purchased from DropSens corporation (Spain), with a 4 mm in diameter working electrode was graphite or modified, the auxiliary and reference electrodes were graphite and Ag/AgCl electrodes, respectively. All of the chemicals used in this investigation were of analytical grade and used without further purification. All solutions were fresh prepared before each test in double distilled water. The crystallinity and phases were characterized by using XRD with Bruker D8 X-ray diffractometer (CuKα; λ=1.5418 Å). An optical property of the nano particles were analyzed using Systronics Double Beam UV–Vis spectrophotometer 2202. The chemical functional group analysis was performing by using Fourier transform infrared spectroscopy (perkin elmer-FTIR spectrum-100) at wave length range of 450-4000 cm-1. The scanning electron microscopy (SEM JEOL-JSM-7600F) and transmission electron microscopy (TEM) were recorded using (JEM-Model 100CX II) to estimate morphological and crystalline properties of samples.

2.2 Synthesis of CeO_2@CuO core-shell nano structures (CeCCS NSs)

Ocimum tenuiflorum leaf with weight of about 20g was taken in double distilled water. Further, the leaves allowed to get dried, 50 ml of distilled water was added to the leaves and boiled it for about 1 hr at temperature 90°C. The extract was filtered with filter paper. To synthesize CeO_2@CuO core-shell nano structures basically followed three factors 1) redox potential of source material 2) stirring time 3) amount of source material. First CeO_2 NPs, 1 m mole of $Ce(NO_3)_2$ was dissolved in 50 ml of distilled water. The leaf extract was added drop wise to the $Ce(NO_3)_2$ solution under constant stirring for 30 min at temperature 120°C to reduce and stabilize the CeO_2 nano suspension. After that, aqueous $Cu(NO_3)_2$ at 0.2 wt% was added drop wise to the above solution at temperature 120°C to obtain CeCCS NSs suspension solution, in which the leaf extract acts as suitable media for transfer and stabilising of CuO over CeO_2 nano particles based on redox potential of precursor solutions. The suspension is stirred for about 6 hrs to obtain final stable product. The obtained CeCCS NSs were centrifuge at 5000 rpm for 15 min and thoroughly washed for three times with ethanol and water respectively, and final resultant product is dried in oven.

To obtain the crystalline shell, the nano particles are calcinated at 450°C. The same procedure has been repeated for 0.4, 0.6 and 0.8 wt% of Cu $(NO_3)_2$. For comparison, CeO_2 and CuO nanoparticles have been synthesized separately using the same procedure.

2.3 Electrode fabrication and electrochemical studies

Homogenous suspension solution were prepared to prepare the modified electrode by ultrasonic technique with the amount of 5 mg of CeCCS NSs were dispersed in 1 ml of distilled water. From the prepared suspension, 4 µl was drop casted on to SPE and dried at room temperature. In the same process the CeO2 (5 mg/ml) and CuO (5mg/ml) were prepared and deposited over other SPE electrodes, respectively. The electrochemical behavior of the sensor electrode was studied using potentiometry at a potential window of 0.0 to +1.0 at various scan rates in 0.1 M NaOH with and without glucose. The electrochemical oxidation of redox peaks is an increase in the concentration of glucose from 1 to 10 mM. Then the optimum potential selected at +0.40 V for ampherometric studies.

3. Result and discussion

The Fig. 1A (line a) represents the characteristic peaks of fluorite cubic CeO_2 (JCPDS file No. 34-0394) corresponding planes located at 28.55^o (111), 33.08^o (200), 47.47^o (220), and 59.08^o (222) angles respectively [Patil et al., 2012]. Fig. 1A (line f) shows diffraction peaks with a phase of monoclinic CuO (JCPDF 45-0937) and main peaks positioned at 35.49°(11-1), 38.73°(111), and 61.53° (11-3), no other impurities such as plant extract, other phases of CuO were observed [Hoa et al., 2010]. From these spectra, we can confirm that the CuO were completely oxidize over crystalline CeO_2 core surface due to the reducing and stabilizing property of leaves extract.

Fig. 1A (lines b-e) the XRD pattern of CeO_2@CuO core-shell nano structures (CeCCS NSs) contains all diffraction peaks of CeO_2 as core with slight decreasing in intensity and for CuO (0.2 to 0.8 wt%) as a shell the intensity of peaks increases, these results shows an indirect proof for the formation of core-shell. Fig. 1B shows the Williamson-hall plot used to provide information on micro strain, which mainly arise due to line broadening and peak shift.

The present bio-mediated synthesis method showed an effect on different structural properties like crystallite size, strain [Suresh et al., 2013; Premkumar et al., 2013], dislocation intensity [Majeed Khan et al., 2011] and specific surface area [Venkateswara Rao et al., 2008], and area of main peaks [Zuo et al., 2013] with the corresponding equations (Eq. 1 to 5) and values are given in Table. 1 (Supplementary information S1). Specifically, the specific surface area was found to be more for 0.4 wt %, which depends on morphology of sample. The estimated crystallite size form Debye scherrer's formula and Williamson- plots were correlated. The plant extract can reduce the dislocation densities, which strongly influence the electro catalytic and electrochemical properties. As the strain is increasing, crystallite size show decrease with increase in peak area of crystal planes and dislocation densities.

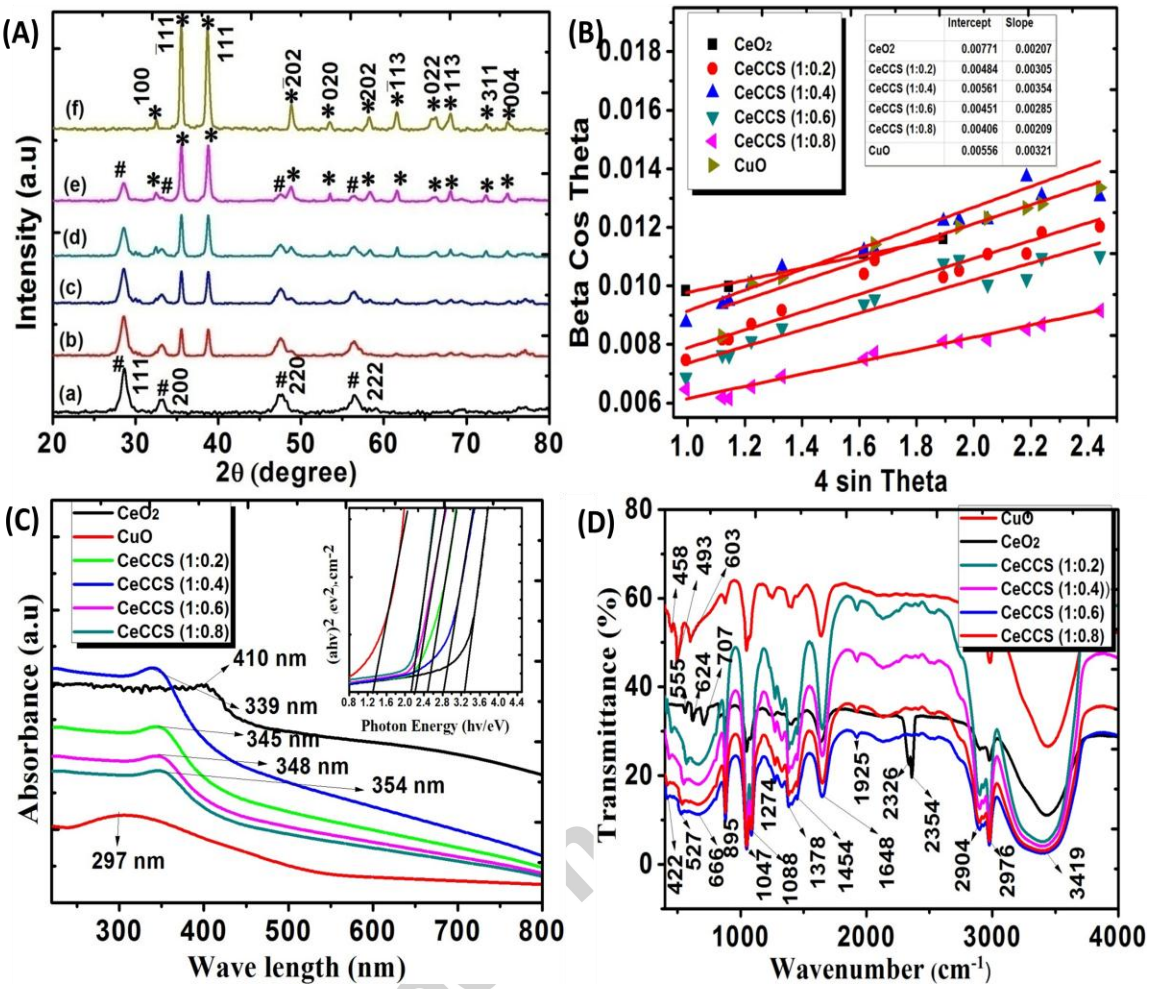

Fig.1. Show the CeO_2, CeCCC (1:0.2), CeCCC (1:0.4), CeCCC (1:0.6), and CeCCC (1:0.8) **A)** XRD. **B)** William and hall son plot. **C)** Uv-Vis graph (inset: energy band gap). **D)** FTIR spectrum.

Fig. 1C displays Uv-Vis absorption spectra (inset: energy bad gap) of pure CeO_2 (410 nm), pure CuO (304 nm) and CeCCS NSs respectively (345, 339, 348, and 354nm) [Rao et al., 2009; Fayaz et al., 2010]. Among the CeCCS NSs, 0.4 wt % (CeCCS) exhibits a blue shift with a band gap of about ~ 2.25 eV due to quantum confinement effect and high absorption intensity of CuO nanoparticles forms thin shell by reducing surface defects on core CeO_2 [Jilie et al., 2007]. The kubelka-munk model [Fan et al., 2008] was employed to estimate optical band gap of CeCCS NSs and estimated values are listed in Table. 2 (Supplementary information S1).

Fig. 1D shows FT-IR spectra of pure CeO_2 -CuO and CeCCS NSs with various atomic weight percentage ranging from 0.2 to 0.8 wt %.The spectra clearly indicate interaction between surface of CeCCS material and ocimum tenuiflourium leaves extract, which contains polyphenols, proteins, acid derivatives and carbohydrates [Singh et al., 2012; Gnanasangeetha et al., 2013]. The Cu-O-H show bending vibrations at wave number about ~ 603 cm^{-1} and Cu-O has stretching vibrations at wave number 493 and 458 cm^{-1} respectively, confirms formation pure CuO phase [Bhatte et al., 2012]. The pure CeO_2 peaks have been observed at 707, 624 and 555 cm^{-1} respectively. From the spectra we observed there is

a shift in peak positions of CeCCS NSs, when compared with pure materials CeO_2 and CuO [Zamari et al., 2012]. The strong broadband peak identified at 3419 cm^{-1} corresponds to O-H stretching vibrations of H bonded alcohols and phenols. The peak shift in O-H stretching vibration presents around 2900 cm^{-1} confirms carboxylic acid. The peak shift at 1648 $cm^{-1}$for N-H is due to bending of primary amines. The aromatic ring structure observed at 1454 cm^{-1} in C-C stretching. Peaks around ~ 2000 and 1378 cm^{-1} shows the involvement of C-N stretching of aromatic amine group of plant extract. The bands at 1200 to 850 cm^{-1} show C-C stretching of alcohols, carboxylic acid, ethers and esters [Jiang et al., 2010]. The combination of bands with peak shift around 800 to 400 cm^{-1} for precursor material could be due to the formation of hydroxyl groups with final confirmation of bio-compounds in plant extract, which intern helps in formation of core-shell nanostructures.

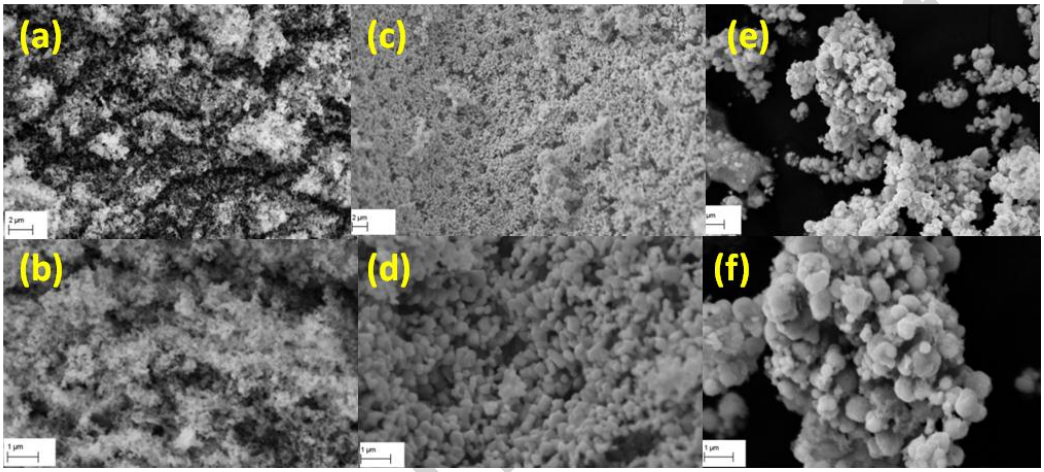

Fig. 2. SEM images of **a, b)** CeO_2. **c, d)** CuO. **e, f)** 0.4 wt % of CeCCS.

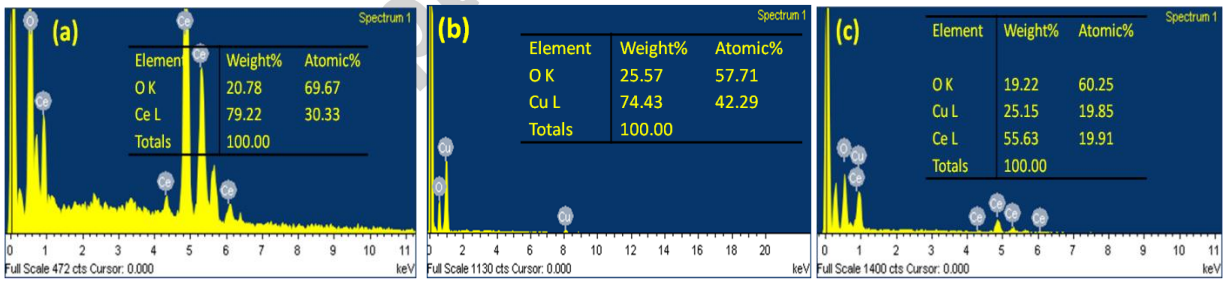

Fig. 3. Shows the EDAX images of a**)** CeO_2. **b)** CuO. **c)** 0.4 wt % of CeCCS.

The data obtained from XRD, Uv-Vis, and FTIR, we done the SEM morphological studies at 2µm and 1 µm magnification as shown in Fig. 2 for pure CeO_2 (a, b), pure CuO (c, d) and 0.4 wt% of CeCCS NSs (e, f). Low-resolution nanostructures of CeCCS exhibit curl structure around each other with numerous irregular shapes with a micrometer size, which are suitably assembled as core-shells. The high-resolution images of CeCCS NSs show a clear structure thickness about micron level with all flexural spherical core-shell structures. Furthermore, SEM micrographs indicate formation of shell (CuO) over

core (CeO_2) truly influences the size, which also reflected in XRD, Uv-Vis, and FTIR results. E-DAX spectra confirms elemental distribution of Ce, Cu, and O components in CeCCS NSs mole ratio equal to 1:0.4 wt % of as shown in Fig. 3. These results indicate core–shell structure is composed of CeO_2 and CuO nanoparticles.

The high resolution transmission electron microscope (HRTEM) image of CCCS (0.4 wt %) NSs is shown in Fig. 4. The complete oxidized samples of CuO shell presents in mono dispersed (spherical in shape) nanostructure with a thickness of about 5 to 8 nm and core particle size varies from 23-26 nm. The contrast difference between core and shell materials confirms formation of core-shell with particle size ~ 30 nm. From the SEAD pattern shown in Fig. 4a (inset) have high and low bright spots in ring patterns indicates that CuO (111) coated over Cu (111) surface, which is a direct proof of formation of core- shell and correlated with result of XRD, Uv-Vis, FTIR and SEM results.

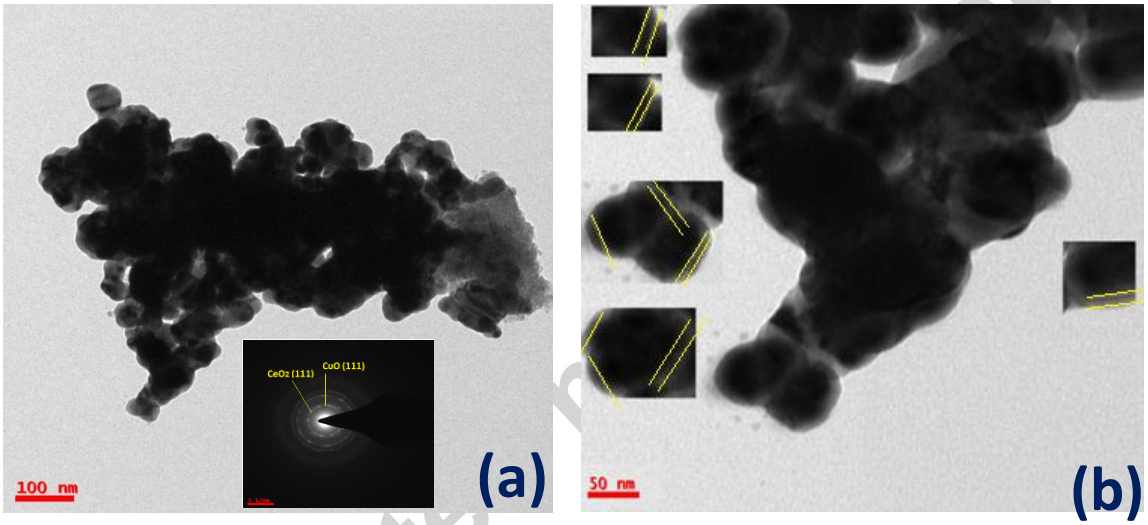

Fig. 4. HRTEM micrographs of 0.4 wt% CeCCS NSs **a)**100 nm **b)** 50 nm magnification.

4. Electrochemical characterization

The cyclic voltameter (CVs) analysis of all the modified electrodes were estimated in 0.1 M of NaOH with a scan rate of 60 mV/s are shown in Fig. 5a, b, c, and d (Supplementary information S1). Fig. 5a shows the bare SPE electrode doesn't have any noticeable redox peaks in the recorded potential range, and in the presence of glucose, exhibits a negligible current. Fig. 5b &c show CeO_2/SPE and CuO/SPE in the presence of 1 mM glucose solution attained a catalytic activity with an observable redox peaks against glucose oxidation in alkaline solution was found to be represents prepared electrode and is useful for glucose sensing phenomena and the negligible redox peaks appeared for without glucose.

Fig. 5d shows CV with 0.4 wt % of CeO_2@CuO core-shell nano structures (CeCCS NSs) electrode has a larger current response compare to current response of CeO_2 and CuO. The core CeO_2 has high conductivity and shell (CuO) has high electro catalytic activity, which in turn can enhance current response in glucose detection. As the thickness of shell layer in nano regim, the results with large specific surface area can provide more reactive sites for redox reaction and electro catalytic activity between CuOand CeO_2 nano particles. Fig. 6a show CVs of CeCCS /SPE at different scan rates (30, 60, 90,

120, 150, 180 210 and 240 mVs^{-1}) in 0.1 mole NaOH solution containing 1 mM glucose. The redox peaks of CVs were clearly seen with rapid and quasi-reversible reaction. The oxidation peak can be seen with a significant positive shift and the reduction peak shifts negatively in Fig. 6b indicating CeCCS NSs has kinetic limitation.

Furthermore, the electron transfer ability between electrolyte and electrode surface with various glucose concentrations ranging from 1 mM to 10 mM were systematically, investigated using CVs in 0.1 M NaOH solution at 60 mVs^{-1} (Fig. 6c), the electrochemical oxidation of anodic peak is increased from +0.39 to + 0.46 V with increase in glucose concentration. The optimum potential +0.40 V has been selected for ampherometric studies. The catalytic oxidation mainly depends on the specific surface area, surface material and particle size, which can provide active sites for redox reaction and electrical signal transmission in CeCCS/SPE. Thus, the synergistic effect can result in improved performance for detection of glucose, indicating that electrode can be applied for detection of glucose.

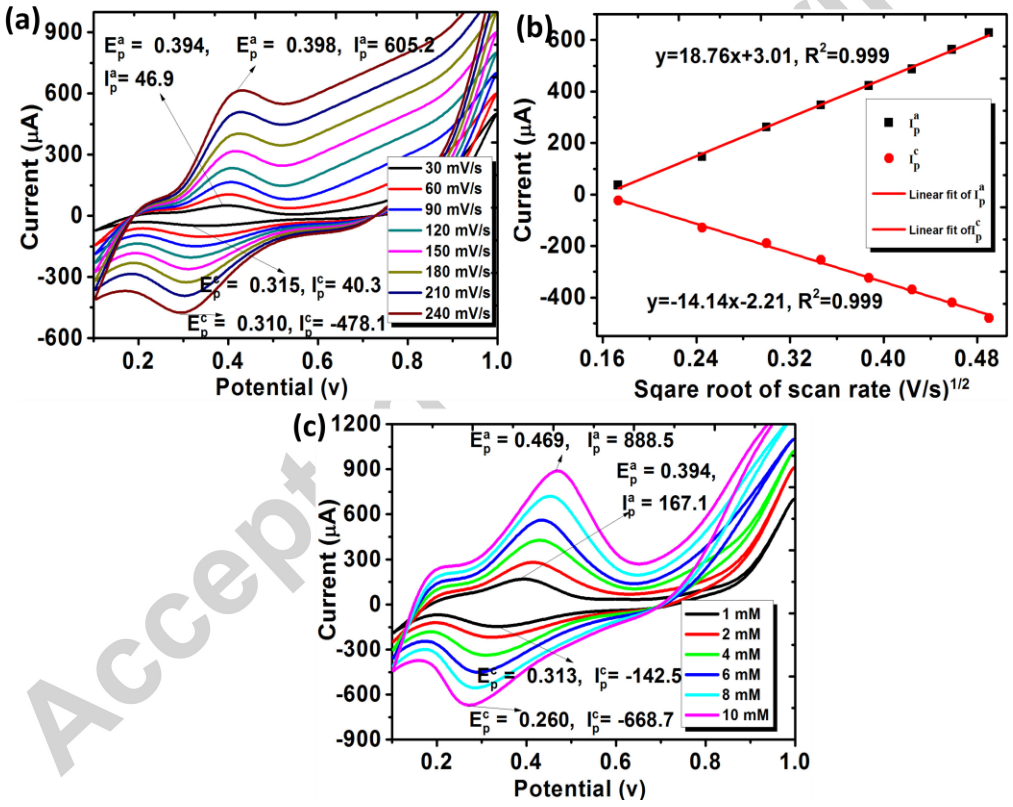

Fig. 6. a) CVs of the CeCCS/SPE at different scan rates (30, 60, 90, 120, 150, 180, 210 and 240 mVs^{-1}).**b)** Square route of different scan rates **c)** CVs of CeCCS/SPE in the presence of 1 to 10 mM glucose concentration.

4.1. Glucose sensing mechanism

The mechanism of glucose sensing by core-shell nanostructures have been described by the following sections, 1) Electrode 2) Electrode surface 3) Interface region. The mechanism mainly involves in three process that are adsorption of hydroxyl group on the surface of nanomaterials, electron transfer from p-

type shell (p - type) to core (n - type) due to difference in band positions, and glucose oxidation process takes place due to conversion of glucose to gluconolactone. To determine the energy band positions we have used theoretical prediction of absolute electro negativity (Pearson absolute electro negativity). The energy level positions of semiconductor at zero charges have been calculated by following the empherical equations (6 and 7) and values are given in Table. 3 (Supplementary information S1).

The built in electric field formed at the interface of core-shell structure the Fermi levels will bend the band position in the depletion layer. In this hybridized core shell nanostructure electron, flows from p-type to n-type semiconductor due to the difference in band positions but the migration of holes has blocked due to the potential barrier as shown in Fig. 7. This is the reason the core-shell hetero structure play an important role in glucose sensing.

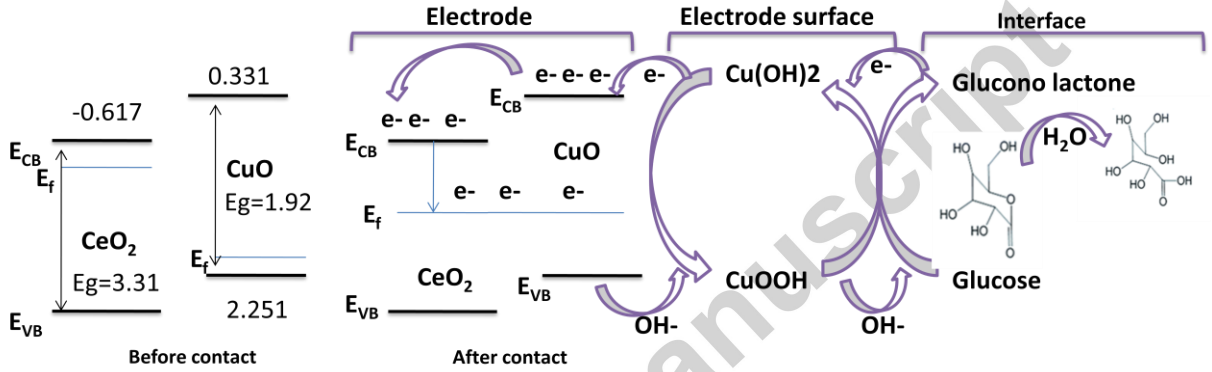

Fig. 7. The energy band positions between CeO_2 and CuO before and after contacting.

Previously, there is a controversy in the exact glucose oxidation mechanism on CuO based electrode in an alkaline medium. However, the oxidation mechanism first proposed by marioli and kuwana [Marioli et al., 1992] and supported by wei et al was most acceptable. The mechanism as follows oxidation occurs from deprotonation of glucose and forms enediol by isomerization, followed by adsorption on electrode surface and oxidation by Cu (II) and Cu (III).

$$CuO + OH^- \rightarrow CuOOH + e^- \quad \ldots\ldots\ldots\ldots\ldots\ldots\ldots (8)$$

$$CuOOH + \text{glucose} + e^- \rightarrow CuO + OH^- + \text{Glucanic acid} \quad \ldots\ldots\ldots\ldots\ldots\ldots (9)$$

At the time of CVs measurement, first the Cu (II) on the CeCCS/SPE modified electrode has oxidized to Cu (III). After wards, the oxidative Cu (III) could catalyze the oxidation of glucose by generating gluconolactone, and further oxidized to gluconic acid as given in Eq (8) and (9). In the non-enzymatic glucose sensing, the Cu (II)/Cu (III) redox couple assisted and increases the current response of the reaction catalyzed by CeCCS/SPE in the presence of glucose.

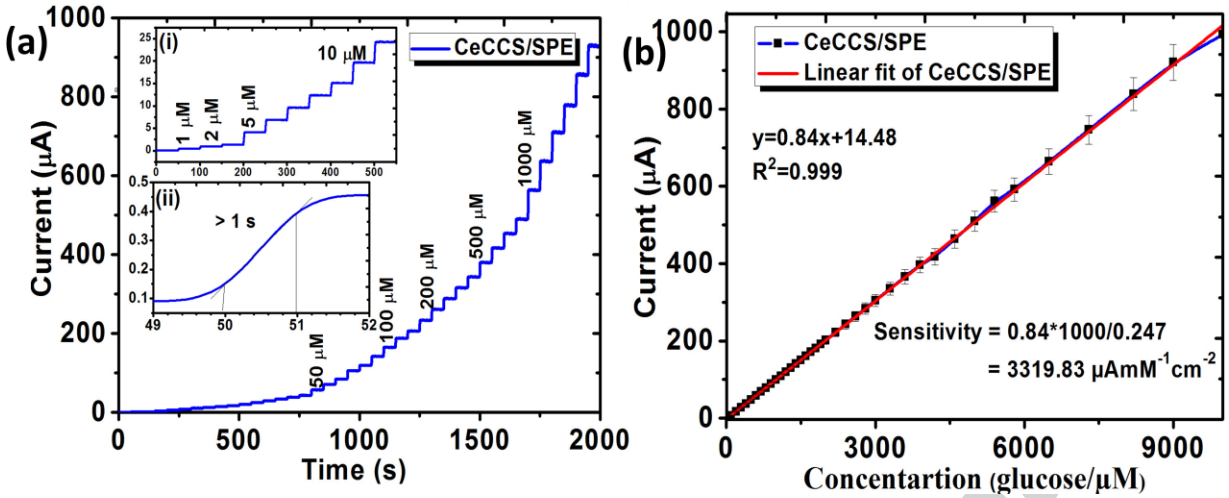

Fig. 8. a) Steady state ampherometric i-t curve (inset: 1-10 µM of glucose).**b)** Calibration plot of steady state current vs. concentration of glucose.

4.2. Amperometric sensing of glucose

Compared to other glucose detection methods, the amperometric methods shows more sensitivity and also provides less noise to signal ratio due to effective mixing of sample solution, convective mass transport and rapid detection towards the oxidation of glucose.

Fig. 8a display the amperometric current response of the non-enzymatic sensing to the successive spiked out glucose concentrations of 9 sets (1, 2, 5, 10, 50,100, 200, 500, 1000 µM) into 0.1 M NaOH at an optimized potential of +0.40 V. The glucose sensor reaches more than 95% steady state current in less than 1 s indicating faster electron communication between glucose and CeCCS/SPE electrode. A fig. 8b display the linear range, low detection limit, and sensitivity have considered from the calibration curve (i-t plot). There was an excellent linear relationship of 1 to 8.9 µM with a sensitivity of 3319.83 $\mu AmM^{-1}cm^{-2}$ and the low detection limit was 0.019 µM. Table. 4 shows the comparison of previously reported effort with the present green synthesis of CeCCS/SPE all these demonstrated that CuO over CeO_2 have been excellent catalytic activity to the oxidation of glucose due the following reasons first, the core shell morphology have large surface area to enhance the more number of active site to the electro catalytic activity of glucose. Second, the CeO_2 core could prove large number of electrons with a good electrochemical redox couple to enhance the electro transfer mechanism with SPE electrode. This reveals that the fabricated non-enzymatic sensor shows excellent performance and sustainable application for glucose sensing.

Table. 4. Comparison of sensing parameters of CeCCS/SPE with other previous reported modified electrodes.

Working electrode	Linear range (µM)	Detection limit (µM)	Sensitivity ($\mu AmM^{-1}cm^{-2}$)	Response time (s)	References
GOx/CeO2/Au	50–400 mg/dL	12.0	0.051	< 5 s	[Ansari et al., 2008]

GOx/CeO2/ITO	2 µM to 6.62 mM	100	0.165	5 s	[Patil et al., 2012]
GOx/CeO2/graphene/FTO	0.05–6.5 mM	2	7.198	-	[Sriparna et al., 2015]
CeO2/Au/CPE	1 to 10 mM	10	57.5	1 s	[Gougis et al., 2014]
CeO2/Au	0.01 to 20 mM	10	44	-	[Gougis et al., 2014]
CuO/CeO2/ITO	-	10	2.77	5~8 s	[Panpan et al., 2016]
CeO2/polyaniline	-	0.56	25.79	6–9 s	[Jie et al., 2013]
CeCCS/SPE	**1 to 8.9 µM**	**0.019**	**3319.83**	**> 1 s**	**Present work**

4.1.1 Reproducibility, Repeatability and Stability

To determine the reproducibility all the electrodes were prepared separately in the same manner and was used to detect the 0.1 M glucose and the calculated RSD values to be 2.39 (n=6) for CeCCS/SPE indicates excellent reproducibility. The RSD of single electrode in six successive measurements was 1.44. This proves the electrode was not poisoned by the oxidation product and can use repeatedly as shown in Fig. 9a (Supplementary information S1). Additionally, the storage stability of prepared CeCCS/SPE was analyzed at room temperature over a period of 2 months (recorded for every 15 days) as shown in Fig. 9b (Supplementary information S1). The peak current of sensors at final day retained a 91.1% of its initial value, revealing the acceptable long-term stability of the sensor due to the excellent adhesion towards electrode and structural stability. The short-term stability estimated after 1-month storage with a RSD value of 96.2 % suggesting the modified electrode incessantly detected glucose without regenerating between each quantity.

4.1.2 Interference tests

Generally, in the human blood the presence of glucose is 30-40 times more than the interference species concentration.

The easily oxidisable compounds such as AA, UA, DA and FA which are normally coexist in human blood with glucose, the obtained results of these compounds shown in Fig. 10a, b, c (Supplementary information S1) have the good current response the CeCCS/SPE has excellent selectivity with an RSD value of 2.66. The sugars were considered to estimate the interference study in 0.1 mM glucose with 0.5 mM sugars. The increase in current response with addition of glucose but the fructose and sorbitol give the similar response with glucose due to the similar structure with the RSD value of 3.25 shows excellent selectivity towards glucose detection. Furthermore, the different chloride ions such as citric acid, KCl, NaCl, KH_2PO_4 and sodium citrate was spiked in glucose to test the chloride poison resistance of CeCCS/SPE modified electrode because in CuO the electro negativity of O is higher than Cl^- ion thus the CuO difficult to form complex structure with chloride ions hence, the modified electrode

have good anti toxicity. The results showed good resistance against chloride ion fouling with RSD valves of 0.19.

4.1.3. Real Sample Analysis

Recovery testing was carried out by standard addition of 1 mM pure glucose to 0.1 M NaOH solutions containing different concentration of human serum and the results were exhibited good agreement with the data measurement by the volunteer's sample (Accu-Check performa) as shown in Table. 5. The recoveries of the proposed method of CeCCS NSs/GCE sensor possessed an excellent accuracy indicating that the prepared working electrode has promising sustainable non-enzymatic biosensor application.

Table. 5. Evaluation of glucose concentration in blood serum sample by CeCCS/SPE electrode.

sample	Serum concentration (mM)	Added glucose (mM)	Found glucose (mM)	Recovery (%)	RSD (%)
1	1.12	1.0	2.11	99.5	1.5
2	2.26	1.0	3.2	98.1	1.9
3	3.35	1.0	4.47	102.7	1.3
4	4.48	1.0	5.79	105.6	1.1

4. Conclusions

In summary, a new non-enzymatic glucose sensing based on CeO_2@CuO core-shell nano structures (CeCCS NSs) were successfully synthesized from ocimum tenuiflourium leaves which acts as reducing and stabilizing agents and the CeCCS/SPE modified electrode was developed. Attributing to high catalytic active and excellent selectivity provided by CuO nanoparticles and high electron transfer rate promoted by CeO_2, this sensor exhibits many attractive analytical features such as high electrocatalytic activity, sensitivity (3319.83 $\mu AmM^{-1}cm^{-2}$), linear range (1 to 8.9 µM), and excellent selectivity. The enhanced performances of CeCCS/SPE make it a promising candidate for glucose sensing.

Acknowledgements

One of the authors, Dayakar. T would like to thank their sincere appreciation to the University Grant Commission (UGC), Government of India for financial support through "Rajiv Gandhi National Fellowship (RGNF)" (F1- 17.1/2013-14/RGNF-2013-14-SC -AND-41054). The author also thanks Centre for Nano Science & Technology (CNST), Institute of Science & Technology (IST), JNTUH, Telangana, India for providing lab and instrumentation facility.

References

Ansari, A.A., Solanki, P.R., Malhotra, B.D., 2008. Appl. Phys. Lett. 92, 263901-3.

A. Horne´s., A. B. Hungrı., P. Bera., A. Lo´pez Ca´mara., M. Ferna´ndez-Garcı., A. Martı´nez-Arias., L. Barrio., M. Estrella., G. Zhou., J. J. Fonseca., J. C. Hanson., and J. A. Rodriguez., 2010. J. AM. CHEM. SOC. 132, 34–35.

Aytekin, Uzunoglu., Dursun, Ali, Kose., Lia, A, Stanciu., Int Nano Lett. DOI 10.1007/s40089-017-0213-3

B, Balamurugan., B, R, Mehta., 2001. Thin Solid Films. 396, 90-96.

D. Gnanasangeetha., D. SaralaThambavani., 2013. Res. J. Mater. Sci. 1, 1.

Fayaz, AM., Balaji, K., Girilal, M., Yadav, R., Kalaichelvan, PT., Venketesan, R., 2010. Nano med Nanotechnol Biol Med. 6, 103–109.

Gougis,M., Pereira, A., Ma, D.L., Mohamedi, M., 2014. RSC Adv. 4, 39955–39961.

Gougis, M., Tabet-Aoul, A., Ma, D.L., Mohamedi, M., 2014. Microchim. Acta. 181, 1207–1214.

Hoa, D. H., Quy, N. Y., Jung, H., Kim, D., Kim, H., Hong, S.K., 2010. Sens. Actuators B 146, 266–272.

H. B. Premkumar., B. S. Ravikumar, D.V. Sunith., H. Nagabushana., S.C. Sharma., S. Mohandas Bhat., B.M. Nagabhushana., R.P.S. Chakradhar., M.B. Savitha., 2013. Spectrochim. Acta, Part A. 115, 234-243.

Huizhi Bao., Zhenhua Zhang., Qing Hua., and Weixin Huang., 2014, Langmuir, dx.doi.org/10.1021/la501406w,

J. C. Fan., and Z. Xie., 2008. J. Mat. Sci. Eng. B. 3, 61-65.

Jilie, K., Shaoning, YU., 2007. Acta Bio chim Bio phys Sin. 39, 549–559.

Jie, Zhang., Panpan, Guan., Yongjian, Li., Wei, Li., and Qingping, Guo., 2016. Bulletin of the korean chemical Society. ISSN (Print) 0253-2964, (Online) 1229-5949.

J. Singh., P. Kumar., K.S. Hui., K.N. Hui., K. Ramam., R.S. Tiwari., O.N. Srivastava., 2012. Cryst Eng Comm. 14, 5898–5904.

J. M. Marioli., T. Kuwana., 1992. Electrochimica Acta. 37, 1187-l 197.

Kun, Li., Guoli, Fan., Lan, Yang., Feng, Li., 2014. Sensors and Actuators B: Chemical. 199, 175-182.

K. Venkateswara Rao., C.S. Sunandana., 2008. Journal of Materials Science. 43, 146-154.

K.D. Bhatte., D.N. Sawant., D.V. Pinjari., A.B. Pandit., B.M. Bhange., 2012. Mater. Lett. 77, 93.

L. C. Jiang., W. D. Zhang., 2010. Biosensor and Bioelectronics. 25, 1402–1407.

M, Heinemann., B, Eifert., C, Heiliger., 2013. Phys. Rev. B. 87, 46-50.

M.A. Majeed Khan., Susil, Kumar., Maqusood, Ahamed., S.A. Alrokayan., M.S. AlSalhi., 2011. Nanoscale Res.Lett. 6, 434.

N, John, Sushma., B, Mahitha., K, Mallikarjuna., B, Deva, Prasad, Raju., 2016. Appl. Phys. A. 122, 544.

Panpan, Guan., Yongjian, Li., Jie, Zhang., and Wei, Li., 2016. Nanomaterials. 6, 159.

P. S. Barbato., S. Colussi., A. Di Benedetto., G. Landi., L. Lisi., J. Llorca., A. Trovarelli.,2016. J. Phys. Chem.120, 13039–13048.

Patil, D.; Dung, N.Q.; Jung, H.; Ahn, S.Y.; Jang, D.M.; Kim, D. Biosens. Bioelectron. 2012, 31, 176–181.

P, Sun., W, Zhao., Y, Cao., Y, Guan., Y, Sun., G, Lu., 2011. Cryst Eng-Comm. 13, 3718–3724.

R. Suresh., V, Ponnuswamy., R. Mariappan., 2013. Appl. Surf, Sci. 273, 457-464.

Rahman, M.M., Ahammad, A.J.S., Jin, J.H., Ahn, S.J., Lee, J.J., 2010. Sensors.

Rupali, S, Patil., Mangesh, R, Kokate., Sanjay, S, Kolekar., 2012. Spectrochimica Acta Part A. 91, 234– 238.

R. Zamari., A. Zakaria., H.A. Ahangar., M. Darroudi., A.K. Zak., G.P.C. Drummen., 2012. J. Alloys Compd. 516, 41.

Shearer, C.J., Cherevan, A., Eder, D., Adv. Mater. 26, 2295–2318.

Shanghong, Zeng., Yan Wang., Suping Ding., Jesper J.H.B. Sattler., Elena Borodina., Lu Zhang., Bert M., Weckhuysen., Haiquan Su., 2014. Journal of Power Sources. 256, 301-311.

Shanghong Zeng., Wenli Zhang., Michał Sliwa., Haiquan Su., 2013. International journal of hydrogen energy. 3 8, 3597-3605.

S.C, Warren., M.R, Perkins., A.M, Adams., M, Kamperman., A.A, Burns., H, Arora., 2012. Nat. Mater. 11, 460–467.

Sriparna, D., Mohanty, S., Nayak, S.K., 2015. Bioprocess. Biosyst. Eng. 38, 1671–1683.

Trovarelli, A., Boaro, M., Rocchini, E., de Leitenburg, C., Dolcetti, G., 2001. J. Alloy. Compd. 323, 584–591.

Tschope, A., Ying, J.Y., 1994. Nanophase Mater.: Synth. Prop. Appl. 260, 781–784.

T.P. Rao., M.C.S. Kumar., S.A. Angayarkanni., M. Ashok., 2009. J. Alloys Compd. 485, 413-417.

Uzunoglu, A., Stanciu, L., 2016. Anal. Chim. Acta. 909, 121–128.

Uzunoglu, A., Zhang, H., Andreescu, S., Stanciu, S., 2015. Springer J. Mater. Sci. 50, 3750–3762.

Wang, Xiao., Dapeng, Liu., Junqi, Li., Jiangman, Zhen., and Hongjie, Zhang., 2015. NPG Asia Materials. 7, 158.

Yan, Zhong., Tielin, Shi., Zhiyong, Liu., Siyi, Cheng., Zirong, Tang., 2016. Sensors and Actuators B: Chemical. 236, 326-333.

Yassien, Temerk., Hossieny, Ibrahim., 2016. Sensors and Actuators B: Chemical. 224, 868-877.

Zuo, Y., Huang, X., Li, L. & Li, G. 2013. J. Mater. Chem. A. 1, 374–380.

Z, Liu., X,D, Wen., X,L, Wu., Y,J, Gao., H,T, Chen., J, Zhu., 2009. J. Am. Chem. Soc. 131, 9405–9412.

Zhuang, Z., Su, X., Yuan, H., Sun, Q., Xiao, D., Choi, M.M.F., 2008. Analyst 133, 126–132.

Highlights

- *Ocimum tenuiflorum* leaf extract were used to prepare Ag@CuO core shell nanostructure
- Structural, optical and morphological properties are studied.
- The ACCS/SPE showed a sensitivity of 3319.83 $\mu AmM^{-1}cm^{-2}$.
- Bio-mediated route synthesized NSs shows sustainable sensing properties.